ISPRS Journal of Photogrammetry and Remote Sensing 70 (2012) 78–87

Contents lists available at SciVerse ScienceDirect

ISPRS Journal of Photogrammetry and Remote Sensing

journal homepage: www.elsevier.com/locate/isprsjprs

Comparison of support vector machine, neural network, and CART algorithms for the land-cover classification using limited training data points

Yang Shao [a,*], Ross S. Lunetta [b]

[a] US Environmental Protection Agency, National Research Council, National Exposure Research Laboratory, 109 T.W. Alexander Drive, Research Triangle Park, NC 27711, USA
[b] US Environmental Protection Agency, National Exposure Research Laboratory, 109, T.W. Alexander Drive, Research Triangle Park, NC 27711, USA

ARTICLE INFO

Article history:
Received 1 September 2011
Received in revised form 7 February 2012
Accepted 2 April 2012
Available online 9 May 2012

Keywords:
Land-cover mapping
Support vector machine
Accuracy assessment

ABSTRACT

Support vector machine (SVM) was applied for land-cover characterization using MODIS time-series data. Classification performance was examined with respect to training sample size, sample variability, and landscape homogeneity (purity). The results were compared to two conventional nonparametric image classification algorithms: multilayer perceptron neural networks (NN) and classification and regression trees (CART). For 2001 MODIS time-series data, SVM generated overall accuracies ranging from 77% to 80% for training sample sizes from 20 to 800 pixels per class, compared to 67–76% and 62–73% for NN and CART, respectively. These results indicated that SVM's had superior generalization capability, particularly with respect to small training sample sizes. There was also less variability of SVM performance when classification trials were repeated using different training sets. Additionally, classification accuracies were directly related to sample homogeneity/heterogeneity. The overall accuracies for the SVM algorithm were 91% (Kappa = 0.77) and 64% (Kappa = 0.34) for homogeneous and heterogeneous pixels, respectively. The inclusion of heterogeneous pixels in the training sample did not increase overall accuracies. Also, the SVM performance was examined for the classification of multiple year MODIS time-series data at annual intervals. Finally, using only the SVM output values, a method was developed to directly classify pixel purity. Approximately 65% of pixels within the Albemarle–Pamlico Basin study area were labeled as "functionally homogeneous" with an overall classification accuracy of 91% (Kappa = 0.79). The results indicated a high potential for regional scale operational land-cover characterization applications.

1. Introduction

MODIS (Moderate Resolution Imaging Spectroradiometer) data has been increasingly used to characterize land-cover and monitor vegetation phenology at regional and global scales, since being launched in 2000. One of the most appealing aspects of MODIS data is its unique combination of spectral, spatial, radiometric, and temporal resolutions; which are considered to be substantially improved over other similar observation systems (Townshend and Justice, 2002). It has become common practice to utilize MODIS time-series data to monitor vegetation characteristics and condition using phenology information and derived metrics that can provide additional information to differentiate spectrally confusing cover types (Defries and Townshend, 1994; Friedl et al., 2002; Loveland et al., 2000). At global scales, Friedl et al. (2002) developed an operational annual land-cover mapping approach using MODIS time-series data. For regional applications, a large number of researchers have been exploring MODIS-based classification protocols (Knight et al., 2006), algorithms (Hansen et al., 2003; Lobell and Asner, 2004), and validation approaches (Giri et al., 2005).

The use of MODIS time-series data, however, can substantially increase data input volume (features/dimensions) for classification applications. For example, many researchers have applied a large number of MODIS spectral and temporal band combinations in their classifications (Carrão et al., 2008; Friedl et al., 2002; Knight et al., 2006; Xavier et al., 2006; Xiao et al., 2005; Wardlow et al., 2007). In addition to the increasing computational requirements, the Hughes phenomenon can also impact classification performance (Bishop, 2006; Camps-Valls et al., 2008; Gualtieri and Cromp, 1999; Melgani and Bruzzone, 2004). Also, the availability of training pixels is often limited in practice, which may reduce the generalization of the classifier. Feature selection can be used to reduce the impact of Hughes phenomenon, but aggressive feature reduction may lead to information loss (Melgani and Bruzzone, 2004). These problems have been widely addressed in hyperspectral remote sensing applications that also use hundreds

* Corresponding author. Address: Department of Geography, Virginia Tech, 115 Major Williams Hall, Blacksburg, VA 24061, USA. Tel.: +1 919 541 4918.
E-mail address: yshao@vt.edu (Y. Shao).

0924-2716/$ - see front matter © 2012 International Society for Photogrammetry and Remote Sensing, Inc. (ISPRS) Published by Elsevier B.V. All rights reserved.
http://dx.doi.org/10.1016/j.isprsjprs.2012.04.001

of input features for image classification and object detection. Recent studies have suggested that support vector machine (SVM) can provide good results for hyperspectral remote sensing classification and superior results have been reported compared to traditional remote sensing classification algorithms such as maximum likelihood (ML), k-nearest neighbor, and neural networks (NN) (Huang et al., 2002; Melgani and Bruzzone, 2004; Pal and Mather, 2005). The most appealing property of SVM was the high capacity for generalization with relatively small numbers of training data points (Bishop, 2006; Pal and Mather, 2005). However, the potential of SVM has not received much attention for MODIS time-series data classification. Specifically, the performance of SVM classification has not been thoroughly assessed with regard to training sample sizes, and training data variations and characteristics (i.e., homogeneous vs. heterogeneous).

The objective of this study was to implement and assess SVM classification performance using MODIS time-series data. We compared SVM approach with the two most commonly used nonparametric classification algorithms: (i) multilayer perceptron neural networks (NN); and (ii) classification and regression trees (CART). The experiment was designed for examining the classification performance using relatively small training samples. We focused on the impact of training sample sizes ranging from 20 to 800 pixels per class using randomly selected samples from a large pool of training data points. Accuracy assessments were performed using multiple independent reference datasets. In addition to the accuracy assessment for pure pixels, we also assessed mixed pixels, because many MODIS pixels (250 m GSD) were generally a mixture of two or more cover types. The research goal was to provide insights for regional scale land-cover classification applications using MODIS time-series data.

2. Background

2.1. SVM classifier

Early development of SVM started in 1970s and the popularity of SVM for pattern recognition and classification is actually surged in the late 1990s (Vapnik, 1995; Vapnik, 1998). In remote sensing, SVM was primarily used for the hyperspectral image classification and object detection (Gualtieri and Cromp, 1999; Melgani and Bruzzone, 2004); although researchers have recently expanding its application for multispectral remote sensing data (Foody and Mathur, 2004; Huang et al., 2002; Pal and Mather, 2005). Melgani and Bruzzone (2004) and Huang et al. (2002) provided a detailed introduction of SVM to the remote sensing community. Mountrakis et al. (2011) summarized empirical results from over 100 articles using the SVM image classification algorithm. The primary advantage of SVM was good generalization capability with limited training samples. The authors acknowledged SVM's limitations in parameter selection and computational requirements. However, SVM provided superior performance compared to most other image classification algorithms for both real-world remote sensing data and simulated experiments.

Using hyperspectral remote sensing data, Melgani and Bruzzone (2004) performed a detailed comparison of SVM, conventional K-nearest neighbor, and a radial basis neural network. Their results indicated that SVM substantially outperformed the other two classifiers. They concluded that SVM was less sensitivity to the Hughes phenomenon, thus feature selection procedure may not be needed for high dimensional dataset. Furthermore, they compared a range of SVM multi-class classification strategies including one-against-all, one-against-one, and hierarchical tree-based classification scheme or approaches. The results from these approaches appeared to be quite similar. The superior performance from SVM was also reported by (Camps-Valls et al., 2004; Camps-Valls and Bruzzone, 2005; Gualtieri and Cromp, 1999), particularly with respect to the classification of hyperspectral remote sensing data.

Huang et al. (2002) implemented SVM classification for a spatially degraded Landsat Thematic Mapper (TM) data. The SVM classification accuracy was superior to that obtained using a maximum likelihood algorithm and a decision tree algorithm. However, there was no advantage to use SVM compared to a neural network classifier. It should be noted that the input feature dimension in their study was rather small. In addition, the sizes of training samples were fairly large (i.e., 2–20% of entire image). The advantage of SVM thus may not be evident in those scenarios. Camps-Valls et al. (2008) presented a novel family of kernel-based methods for time-series image classification. The SVM approach demonstrated superior performance compared to neural networks for high dimension time-series spectral data from multiple sensors. Similarly, Bovolo et al. (2010) approached image change detection as an outlier detection problem. SVM provided a robust outlier detection capability in their study. Carrão et al. (2008) employed SVM to examine the impacts of MODIS temporal and spectral factors for a general land-cover classification in Portugal. Their findings indicated that a limited number ($n = 3$) of MODIS composited images, if selected appropriately, provided sufficient image classification accuracy. The results were consistent with those presented by Shao and Lunetta (2011).

In addition to the SVM-based categorical classification, there is also growing interests in the SVM regression for estimating subpixel land cover proportions (Brown et al., 2000). In general, the SVM represents a novel approach compared to conventional ML, CART, and NN classifiers. Currently, only a few studies have applied SVM algorithm for time-series MODIS image classification (Carrão et al., 2008). Additional SVM applications for regional scale land-cover classification need to be conducted to better understand performance. The implementation of SVM for MODIS time-series data is of particular interest for operational regional-scale land cover characterization.

2.2. NN and CART classifications

Neural network classification algorithms have long been used for remote sensing image classification (Paola and Schowengerdt, 1995; Richards and Jia, 1999). Many have suggested that these types of models are superior to traditional statistical classification approaches (i.e., maximum-likelihood classification), because they do not make assumptions about the nature of data distribution, and the function is simply learned from training samples. Several neural network models are commonly applied (Tasdemir and Merenyi, 2009). ARTMAP models have been increasingly used due to their stability and computational performance (Carpenter et al., 1997). For instance, Gopal et al. (1999) used fuzzy ARTMAP to classify annual sequence of composited NDVI data. They found an increase of 7.0% in overall accuracy compared to a maximum likelihood classification. The same ARTMAP algorithm was also used by other researchers for time-series NDVI image classification at regional and global scales. The results from ARTMAP algorithm were consistently superior to those obtained from a maximum likelihood classification. Bagan et al. (2005) employed the self-organizing map (SOM) neural network technique to classify land-cover types using 16-day composites of MODIS Enhanced Vegetation Index (EVI) data. Superior classification results were found compared with those obtained using maximum likelihood classification method. Using time-series MODIS NDVI data, Shao et al. (2010) characterized specific crop types with a multi-layer perceptron (MLP) neural network model. The principal challenges associated with MLP implementation was the adjustment of network parameters (network architecture, learning rate, and momentum).

Early stopping criteria are also needed to reduce the risk of network overfitting (Bishop, 2006).

CART (Breiman et al., 1984) is a tree-based framework that has been widely used in remote sensing applications (Friedl et al., 2002; Lawrence and Wright, 2001). The key to determine the structure of a decision tree is to select an input feature and threshold value at each splitting. The CART can easily result in overfitting if allowed to grow to fit the training data. A tree prune can be employed to cut tree levels, thus increase the generalization ability of CART (Lawrence and Wright, 2001; Venables, 1997). Currently, this type of tree-based classification algorithm is the dominant technique for MODIS and TM based classifications. The standard MODIS global land-cover data is produced by the decision-tree algorithm, because of its robustness and global operational considerations (Friedl et al., 2002; Quinlan, 1993). Using regression tree algorithm, Hansen et al. (2003) examined the continuous field (i.e., sub-pixel land-cover proportions) representations based on signatures from the MODIS time-series metrics. A total of 68 annual metrics were derived from MODIS spectral bands to capture the phonologic cycle. The large number of input feature requires a significant amount of training pixels to generate robust classification result. The CART algorithm was also used by Wardlow and Egbert (2008) to examine the applicability of time-series MODIS 250 m NDVI data for large-area cropland mapping over the US Central Great Plains. The composite MODIS NDVI data were obtained from March 22 to November 1. They obtained very high overall accuracies for general cropland (94%) and summer crop (84%).

3. Methods

3.1. Study area and data pre-processing

The experiment was conducted for the Albemarle-Pamlico Estuarine System (APES) in North Carolina and Virginia (Fig. 1), US. The APES covers an area of 52,000 km^2 and is the second largest estuarine system in the US. The land-cover types and compositions of APES are considered to be representative for the southeastern US. For the last 10–15 years, numerous remote sensing dataset, field observation, and water quality indicators have been collected for the APES. It is treated as a Near-Laboratory research area by US Environmental Protection Agency (EPA) to monitor long-term landscape change, water quality, and watershed conditions (Knight et al., 2006; Lunetta et al., 2006).

The MODIS 16-day composite of vegetation index data (MOD13Q1, Collection 5) from 2000 to 2009 were obtained from the USGS EROS Data Center (http://eros.usgs.gov/). The spatial resolution for this MODIS dataset is 250-m. Each composite image contains 13 data layers that represent MODIS-derived vegetation index, data quality, and acquisition information. For this research, the EVI (Enhanced Vegetation Index) was selected over NDVI (Normalized Difference Vegetation Index) for the image classification, because EVI has fewer problems with saturation and provides better separability between cover types (Huete et al., 2002). In addition to the EVI, the short wave infrared (SWIR) surface reflectance band-7 was also included as input, because it can provide useful information to differentiate urban and agricultural land. The MODIS reliability index was used to identify pixels with quality issues. The MODIS reliability index is a simple decimal number that ranks the product into several data quality categories (i.e., good, marginal, etc.). Overall, the image quality is quite good for the APES. Generally, pixels identified as good and acceptable quality are over 95% of total pixels for all composite images. A Savitzky–Golay filter was applied to estimate new values for pixels with poor reliability index (Chen et al., 2004). The 16-day MODIS composite time-series data were re-projected from a sinusoidal projection into an Alber's Equal Area Conic projection. For each calendar year, a total of 46 input features (23 EVI and 23 MIR bands) were used for the image classification.

The NLCD (National Land Cover Dataset) 2001 data were also obtained from the USGS EROS Data Center. A geographic link between the MODIS and NLCD 2001 data were developed. For each 250 m MODIS pixel, we computed the proportional land-cover for major NLCD 2001 classes including urban, deciduous forest, evergreen forest, agricultural land, and wetland. The urban class is combined from four NLCD 2001 sub-classes: open space, low intensity, medium intensity, and high intensity impervious surface. The pasture/hay and cultivated crop classes in NLCD 2001 were combined as a single group of agricultural land. A few cover classes such as barren land, mixed forest, and scrub/shrub were discarded due to their limited area coverage (i.e., <1.0%) in the study area. In addition, all water pixels in the MODIS data were masked out using the NLCD 2001 as reference (i.e., >50% as threshold). The main reason was that MODIS time-series data for water pixels had inconsistent values. The values for water pixels can be affected by cloud presence during the temporal compositing process. This may cause large uncertainties for the image classification (Knight et al., 2006; Lunetta et al., 2010). The spatial scaling-up of NLCD 2001 provided detailed sub-pixel cover type proportions at the 250 m MODIS spatial scale.

A large number of training and validation pixels were derived by linking 2001 NLCD and MODIS dataset. Classification accuracy and error assessment were also examined based on the characteristics of NLCD 2001 reference data. Furthermore, these cover types could be flexibly grouped into broad classes for different applications. For the general comparison of SVM, NN, and CART, a simplified broad land-cover classification scheme was used in this study: urban, natural land, and agricultural land. The natural land includes deciduous forest, evergreen forest, and wetland. It should be noted that NLCD 2001 itself has classification errors and uncertainties (Nowak and Greenfield, 2010; Wickham et al., 2010). Wickham et al. (2010) conducted a detailed accuracy assessment for the NLCD 2001 data that documented an overall accuracy of 85.3% (Anderson Level I). In this study, the NLCD 2001 classes were aggregated to three broad classes. This would potentially increase the overall accuracy of reference data and support general accuracy assessment at coarser spatial resolution (i.e., 250 m). Past research has indicated that finer resolution satellite derived land-cover classification products can provide reference data comparable to those derived from aerial photography interpretation to evaluate coarser resolution imagery products (Lunetta et al., 2002).

3.2. SVM classification

MODIS pixels with 100% singe class cover proportion (i.e., 100% urban) were considered homogeneous pixels. Within the broad classification scheme, a large number of pure pixels were identified for the APES study region. Overall, approximately 24% of MODIS pixels were determined to be homogeneous for year 2001. To examine the impact of training sample size on classification results, we generated a number of training datasets with different training sample sizes: 20, 50, 100, 200, 300, 400, 500, 600, 700, and 800 pixels for each cover type. We repeated the random selection of training samples 50 times. This allowed us to examine the robustness of classification algorithms with respect to the variability of training dataset.

The SVM$_{light}$ package was used for the MODIS data classification (Joachims, 2002). We used a one-against-all approach for the multi-class classification problem. For example, an urban-against-all classifier was designed to separate urban class against the remaining cover types. Therefore, we decomposed the multi-class problem into three two-class classification problems: urban-against-other, natural land-against-other, and agricultural land-against-other.

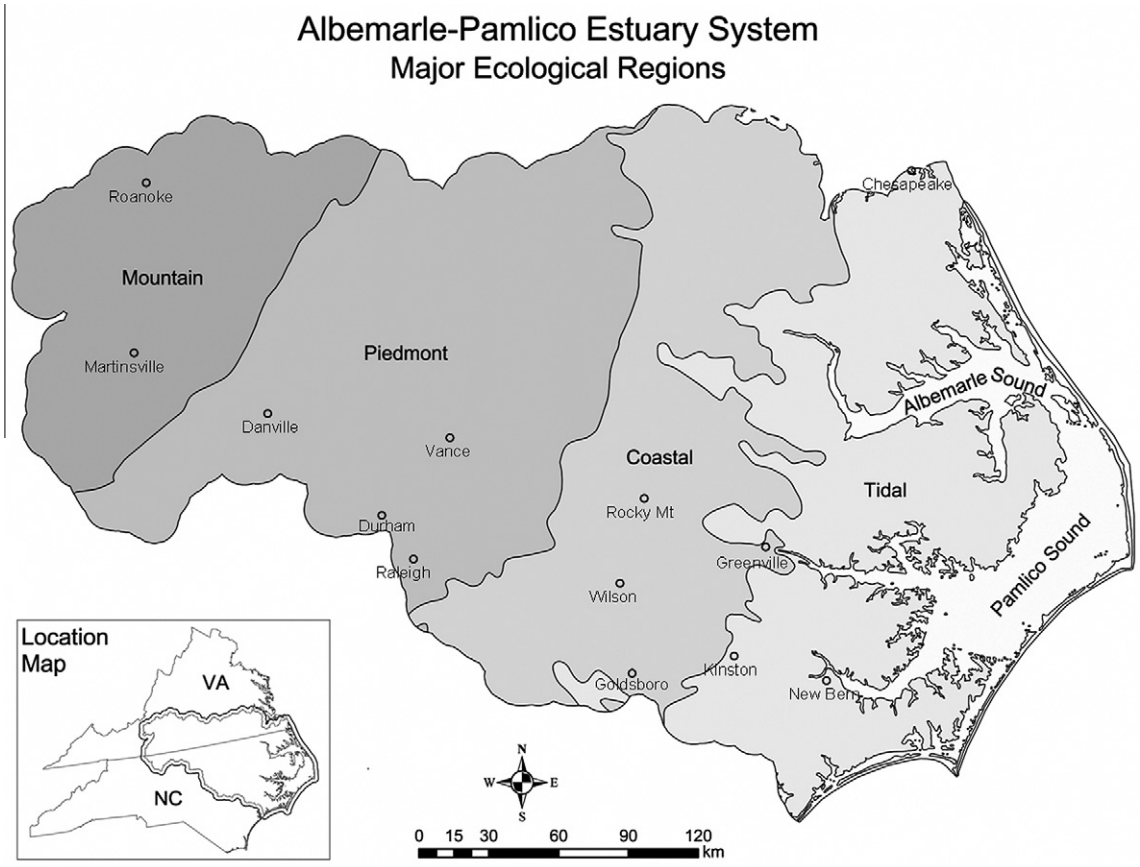

Fig. 1. Location map of the Albemarle-Pamlico Estuary System (APES) study area.

Each two-class classifier was trained to separate one class of interest and the "other" class combined from the remaining two classes. Accordingly, there were three output values for each pixel. We predicted the final class label based on the largest output value among the three. Although the one-against-all approach may suffer from training set imbalance and output scaling problems, it's currently the most common SVM approach due to its simplicity and efficiency (Bishop, 2006).

The MODIS time-series data were rescaled (0.0–1.0) for the SVM training. A radial basis function (RBF) was selected as the primary SVM kernel function. A range of values were tested for two SVM parameters C (1–50) and γ (0.1–10). A grid-search method was used to examine various combinations of C and γ values, and the best combination was identified using a cross-validation method (Joachims, 2002). Specifically, for each training dataset, 20% training pixels were set aside for the cross-validation purposes. After training, the MODIS time-series data were used as input to produce classification maps for the entire study area. This type of cross-validation approach was also implemented for the other two classification algorithm. This was important for the consistency and comparison purposes.

3.3. Neural network and CART classifications

The same training datasets were used for the MLP NN and CART classifications. The software employed for the MLP classification was the Stuttgart Neural Network Simulator (Zell, 1998). A three-layer MLP NN classifier was designed for the classification. The input layer consisted of 46 inputs nodes, indicating 46 input features from MODIS time-series data. For the multiclass MLP classification, three output nodes were used at the output layer, representing three land cover types identified above. Network output target was set as a 1-of-M target coding system (e.g. 1, 0, 0). The number of nodes at hidden layer was examined ranging from 5 to 25. A back-propagation algorithm was used to adjust the weights and minimize the overall error. Different learning rates (0.01–0.20) and momentum values (0.5–0.9) were also tested to identify appropriate network training protocols. The best network architecture and training parameters were identified by a cross-validation approach. For all training dataset, 20% training pixels were set aside for the cross-validation purposes. A trained NN was then used to classify the MODIS time-series image. Ideally, the network output signals would approximate posterior probabilities of three cover classes, if large number of training pixels were employed in the network training.

For the training of the CART algorithm, the three target cover classes were labeled as categorical values of 1–3, respectively. CART splits the MODIS input data into independent regions based on binary decisions. The tree prune was conducted based on a cross-validation method with 20% training pixels setting aside for the cross-validation. The best classification tree was retained for the actual MODIS time-series analysis. It should be noted that the performance of CART algorithm can be improved by bagging and boosting algorithms (Friedl et al., 2002), however, these algorithms were not implemented because they can be applied to each of the three classification methods and potentially improve classification performance for all three methods.

3.4. Accuracy assessment

Five percent of the MODIS pixels were randomly selected for the accuracy assessment after training pixels used for the classification

training were removed from the MODIS pixel pool. To assess classification stability, we conducted accuracy assessments using three different groups of reference data points. For the first group, all randomly selected pixels (5.0% of total pixel) were used for the assessment. The reference pixel was labeled based on the class with the largest sub-pixel portion. For the second group, only pixels with a dominant sub-pixel cover type proportion (i.e., >75%) were used for the accuracy assessment. Accordingly, the accuracy statistics represented classification performance for relatively "homogeneous" pixels. For the third group, the remaining "heterogeneous" pixels (i.e., dominant cover <75%) were used for the accuracy assessment. Accuracy statistics such as overall accuracy and Kappa coefficient were compared for three classification methods with respect to different groups of reference data. The McNemar's significance testing was used to evaluate significant differences between classification methods.

We anticipated large difference in classification accuracy for "homogeneous" versus "heterogeneous" pixel groups. In general, homogeneous pixels should have high accuracy and confidence, while heterogeneous pixels commonly exhibit high classification uncertainties and lower accuracies. To account for this accuracy disparity, we applied a two-level classification labeling approach. In addition to providing a single (or dominant) class label for each pixel, we developed an additional label as pixel purity. The approach was designed to provide additional details about the output signals from classification algorithm. In a neural network-based image classification framework, many studies suggested that the network output signals can be linked to sub-pixel cover proportions (Foody, 1996; Moody et al., 1996). The network output signals can be retained in a "fuzzy" manner (i.e., between 0 and 1). These signals could also be used as a pixel purity index. Similarly, for SVM algorithm, we derived the pixel purity information based on the output signals from the SVM analysis. Specifically, a pixel was labeled as "homogeneous" if the largest SVM output value was >1.0 and the second largest output <1.0. Other pixels were labeled as "heterogeneous" because there was no dominant cover class based on the SVM output values.

4. Results and discussion

4.1. Training sample size and classification repeatability

Fig. 2 shows the overall accuracies and Kappa coefficients for three classification algorithms using a numbers of training sample sizes. For each training sample size, the classification was repeated for 50 trials using different training sets. The solid lines indicate the average accuracy statistics from the 50 trials and the box boundary represent the standard deviation away from the mean value. Overall accuracies clearly show that SVM outperformed NN and CART at the entire range of the training sample sizes. For a smaller training size (i.e., 20 pixels per class), the overall accuracy for SVM was 77%, which was substantially higher than those obtained from the NN (67%) and CART (62%) classification. The difference of overall accuracies for three algorithms reduce as the training sample size increases, although the SVM algorithm still outperformed the NN (−4%) and CART (−7%) at 800 pixels per class. It is also noticeable that the impacts of training sample size were much less for the SVM algorithm compared to the other classification algorithms. For the SVM approach, the overall accuracies achieved at 20 and 800 pixels per class differed by approximately 3%. For NN and the CART approaches, the differences were 9% and 11%, respectively. This suggested that SVM is less sensitive to the training sample size. It can achieve relatively high accuracy even with small number of training pixels (i.e., 20 pixels per class). The result is supported by previous efforts (Melgani and Bruzzone, 2004; Pal and Mather, 2005).

For any given training sample size, smaller variability between individual trials for the SVM compared to the NN and the CART algorithms were evident. For SVM, the variability of the overall accuracy was slightly higher at 20 pixels per class compared to 800 pixels per class. For the NN and the CART algorithms, however, the standard deviation was approximately 8.0% when small training sample size was used. The variability of overall accuracy decreased as the training sample size increased. Kappa coefficients show the same trends as the overall accuracy. The McNemar's significance testing suggested that SVM generated significantly ($p < 0.05$) better results than the CART algorithm for all classification trials (i.e., 20–800 training pixels per class). The comparison of SVM and NN suggested that the results from SVM were significantly better for a majority of trials (467 of 500), the difference between these two algorithms decreases as the size of training sample increases.

The comparison of accuracy statistics indicates that SVM algorithm should be favored among the three classification algorithms, especially when limited numbers of training pixels are available for the classification training. The decreased variability between individual trials is also important in practice, because the selection of training samples can be resource intensive and subjective; different image analyst may choose very different spatial locations to identify training pixels. SVM provided superior and more consistent classification results among the three classification algorithms.

Table 1 shows the error matrix of accuracy assessments using the NLCD 2001 as reference. For simplicity, the results were reported only for experiments using 800 training pixels per class. The reference pixels (250 m GSD) were labeled based on the largest or dominant sub-pixel cover type proportions. Fig. 3 shows the classification results from three algorithms. For all three classification approaches, there were considerable classification errors for urban class. The commission error statistics were 59%, 77%, and 79% for SVM, NN, and CART, respectively. Large overestimation of urban class was particularly evident for NN and CART approaches. The confusion was contributed from the agricultural land. At 250 m spatial resolution, the urban class often has high level of spectral heterogeneity. Generally, residential areas represent various mixtures of vegetation and partial impervious cover. Depending on the mixture level, the temporal signal of urban class can mimic those of agricultural land, causing classification errors (Shao et al., 2010).

The classification accuracies for natural and agricultural lands were much higher than urban class for all three classification algorithms. For natural land, the user's accuracies were 86%, 90%, and 87% for SVM, NN, and CART, respectively. Relatively low and balanced commission/omission errors were observed suggesting good classification performance for all three algorithms. For agricultural land, the commission errors were similar for SVM (27%) and NN (24%); both are much lower than the CART algorithm (33%). There were large differences in the omission errors for three algorithms (SVM = 33%, NN = 38%, and CART = 41%). The relatively high omission error can also be observed in Fig. 3. Many small patches of agricultural land in the mid-west portion of the study area were miss-classified. These results are consistent with past findings in Shao et al. (2010), the patch sizes of agricultural land have significant impacts on the classification accuracies.

The comparison suggested that SVM has major advantages for the urban and agricultural land classification, although there were still substantial omission errors related to these two cover types. For the same study area, Knight et al. (2006) also reported high omission errors using the Spectral Angle Mapper (SAM) algorithm. For urban class, their omission error reached as high as 90%.

4.2. Accuracy for "homogeneous" and "heterogeneous" pixels

It should be noted that the classification performance is not only depending on the training data and classification algorithm.

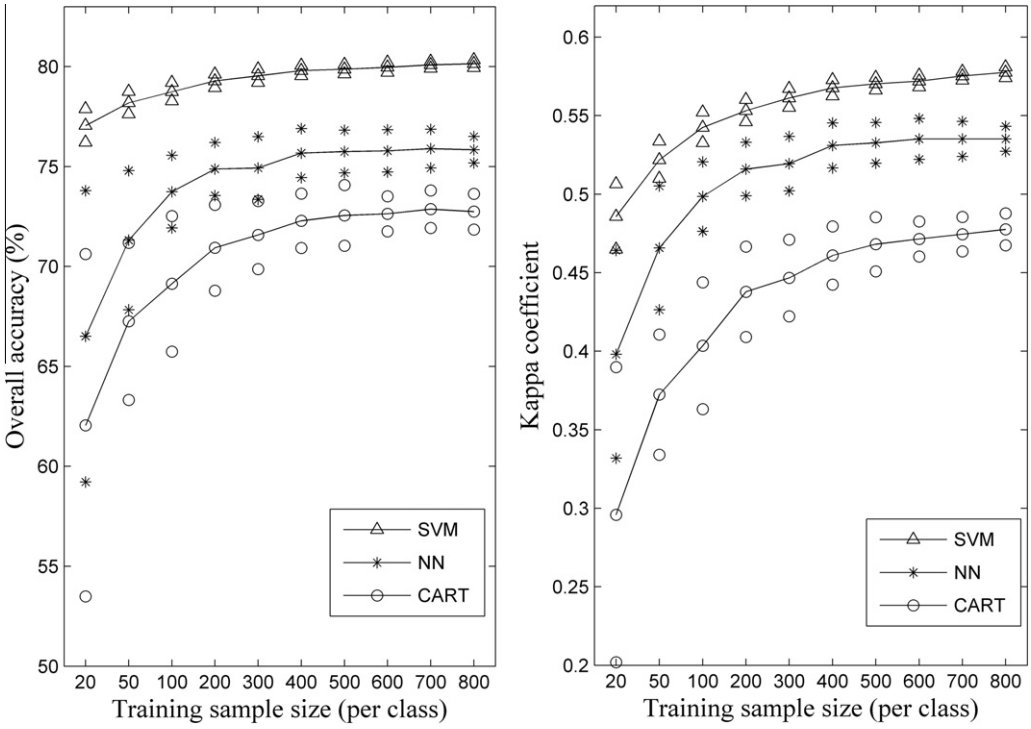

Fig. 2. Comparison of overall classification performance for the SVM, NN, and CART algorithms using a range of training data sample sizes. The solid lines represent mean values and the boundary box indicates one standard deviation bounds.

Table 1
Error matrices were constructed using reference data derived from the NLCD 2001. Pixels were rescaled to 250 m GSD and labeled according to dominant cover type. Five percent of the MODIS pixels were randomly selected for the accuracy assessment.

	Reference					
	Urban	Forest	Ag	Total	% Correct	% Commission
SVM						
Urban	**2.2**	1.4	1.8	5.4	41	59
Forest	1.6	**58.6**	7.9	68.1	86	14
Ag	1.0	6.2	**19.4**	26.5	73	27
Total%	4.8	66.1	29.1	100.0	**80**	(***n*** **= 71,063**)
% Correct	46	89	67			
% Omission	54	11	33			**Kappa = 0.58**
NN						
Urban	**3.4**	6.0	5.7	15.1	23	77
Forest	0.8	**55.0**	5.5	61.2	90	10
Ag	0.6	5.2	**17.9**	23.7	76	24
Total%	4.8	66.1	29.1	100.0	**76**	(***n*** **= 71,063**)
% Correct	72	83	62			
% Omission	28	17	38			**Kappa = 0.54**
CART						
Urban	**3.0**	6.0	5.2	14.2	21	79
Forest	0.9	**52.4**	6.7	59.9	87	13
Ag	0.8	7.7	**17.3**	25.8	67	33
Total%	4.8	66.1	29.1	100.0	**73**	(***n*** **= 71,063**)
% Correct	64	79	59			
% Omission	36	21	41			**Kappa = 0.48**

The characteristics of study area, classification scheme, pixel spatial resolution, and quality of reference data may contribute substantially to the accuracy statistics. Generally, accuracy statistics appear to be "good" if homogeneous pixels are used as reference. Table 2 shows the error matrix using relatively homogenous pixels (dominant cover >75%) as reference. This reduced the total reference pixel number from 71 063 to 42 350. The overall accuracy increased to 91%, 89%, and 85% for SVM, NN, and CART algorithms, respectively. These values are considerably higher than the numbers reported in Table 1. The omission errors for urban and agricultural land were much reduced. Kappa coefficients were also increased substantially to 0.77, 0.74, and 0.65 for three algorithms, respectively. The accuracy statistics appeared to be acceptable, especially the numbers for the SVM algorithm.

Table 3 shows the classification error distributions using only heterogeneous pixels. Although these pixels do not have dominant sub-pixel cover proportions, they still need to be labeled as only one cover classes to provide a traditional hard label approach. The overall accuracies dropped to 64%, 58%, and 55% for SVM, NN, and CART, respectively. The commission and omission errors were very high for the urban class for all three algorithms. This suggests that it is a major challenge to identify urban pixels with relatively high level of pixel heterogeneity. An urban pixel can not be easily identified if the sub-pixel urban proportion is <75%. There was also large confusion between natural and agricultural land; similar results were previously reported by (Friedl et al., 2002). However, SVM and NN performed better than the CART in differentiating these two classes – indicated by the lower omission errors.

Clearly, the characteristics of the reference data are critical for the accuracy statistics. The overall accuracies for "homogenous" and "heterogeneous" pixels differed greatly. For CART algorithm the difference was about 30%. For many remote sensing image classification accuracy assessments, only homogenous pixels are used as reference, thus the overall accuracy may be skewed. Using the SVM approach, we further implemented a two-level classification labeling approach that included a pixel purity label for each pixel based on the SVM output signals (i.e., using threshold value of 1.0). As a result, approximately 65% of total pixels were labeled as "functionally homogeneous" pixels because their largest SVM output values were >1.0 and the second largest SVM output values were <1.0. The overall accuracy for these SVM-derived "homogeneous" pixels were 91% (Kappa = 0.79). Furthermore, a comparison of the SVM-derived "homogeneous" pixels with the NLCD 2001 data indicated that over 77% of these pixels contained dominant sub-pixel cover proportions (>75%), and almost all the remaining

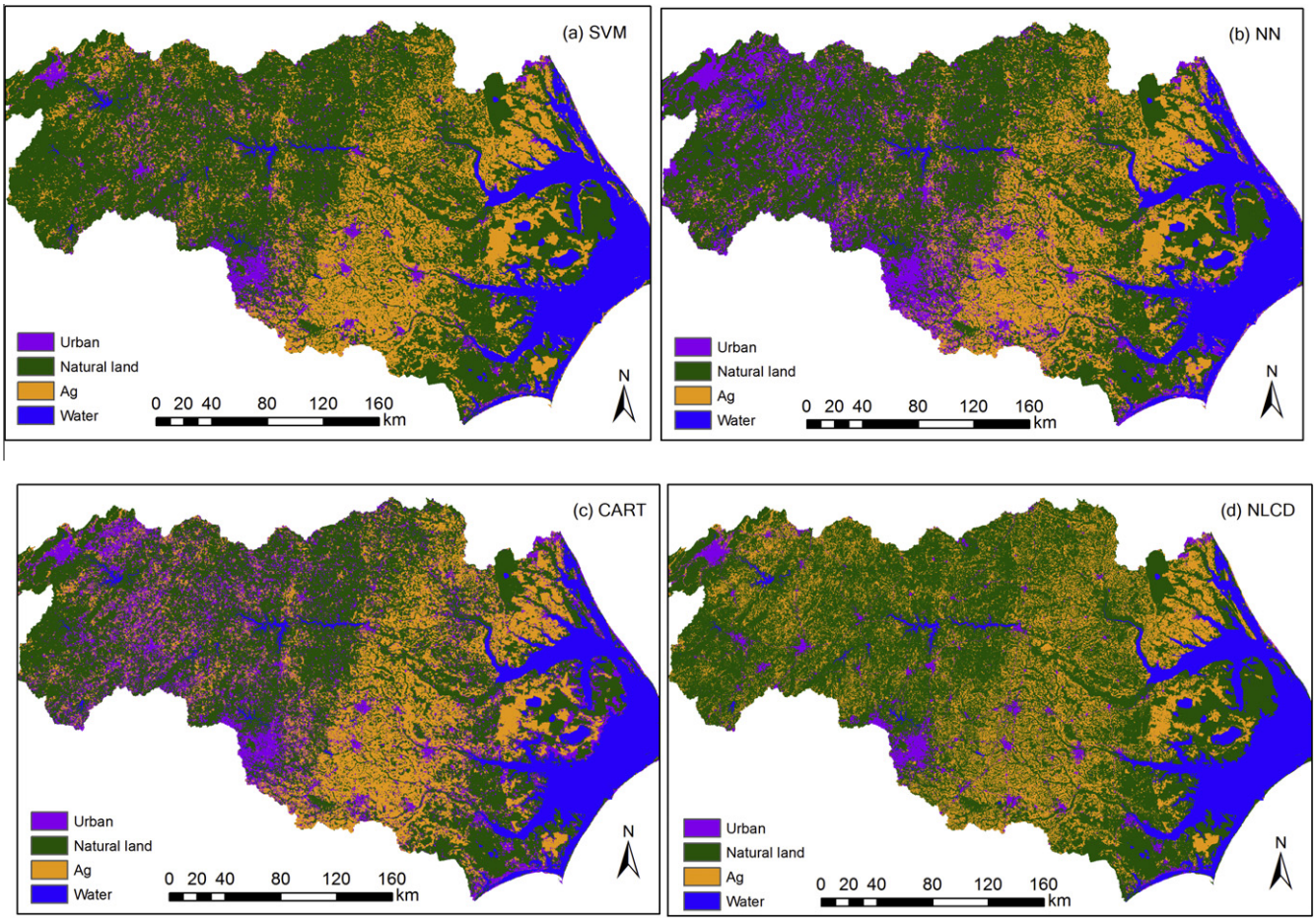

Fig. 3. Comparison of classification results for SVM (a), NN (b), and CART (c) algorithms. The NLCD 2001 (d) is also included as reference.

Table 2
Error matrices were constructed using reference data derived from the NLCD 2001. Pixels were rescaled to 250 m GSD. Only homogenous (>75%) pixels are used as reference data points.

	Reference					
	Urban	Forest	Ag	Total	% Correct	% Commission
SVM						
Urban	**2.4**	1.2	1.0	4.6	52	48
Forest	0.7	**70.6**	2.7	74.0	95	5
Ag	0.3	3.2	**17.9**	21.4	84	16
Total%	3.4	75.1	21.5	100.0	**91**	(***n*** **= 42,350**)
% Correct	69	94	83			
% Omission	31	6	17			**Kappa = 0.77**
NN						
Urban	**3.1**	3.9	2.8	9.7	32	68
Forest	0.2	**68.7**	1.7	70.6	97	3
Ag	0.1	2.5	**17.1**	19.7	87	13
Total%	3.4	75.1	21.5	100.0	**89**	(***n*** **= 42,350**)
% Correct	91	92	79			
% Omission	9	8	21			**Kappa = 0.74**
CART						
Urban	**2.9**	4.2	2.8	9.8	29	71
Forest	0.3	**65.8**	2.7	68.7	96	4
Ag	0.3	5.1	**16.1**	21.4	75	25
Total%	3.4	75.1	21.5	100.0	**85**	(***n*** **= 42,350**)
% Correct	83	88	75			
% Omission	17	12	25			**Kappa = 0.65**

Table 3
Error matrices using the NLCD 2001 as reference data. Note that pixels were rescaled to 250 m GSD. Only heterogeneous (<75%) pixels are used as reference data points.

	Reference					
	Urban	Forest	Ag	Total	% Correct	% Commission
SVM						
Urban	**1.9**	2.0	3.0	6.9	28	72
Forest	2.8	**40.9**	15.5	59.2	69	31
Ag	1.9	10.6	**21.4**	33.8	63	37
Total%	6.6	53.5	39.8	100.0	**64**	(***n*** **= 28,713**)
% Correct	29	76	54			
% Omission	71	24	46			**Kappa = 0.34**
NN						
Urban	**3.8**	9.6	10.0	23.5	16	84
Forest	1.6	**34.8**	10.9	47.3	74	26
Ag	1.2	9.1	**19.0**	29.2	65	35
Total%	6.6	53.5	39.8	100.0	**58**	(***n*** **= 28,713**)
% Correct	58	65	48			
% Omission	42	35	52			**Kappa = 0.31**
CART						
Urban	**3.3**	9.1	8.7	21.0	16	84
Forest	1.7	**33.0**	12.3	47.0	70	30
Ag	1.6	11.5	**18.9**	31.9	59	41
Total%	6.6	53.5	39.8	100.0	**55**	(***n*** **= 28,713**)
% Correct	49	62	47			
% Omission	51	38	53			**Kappa = 0.26**

pixels had a relatively high level of homogeneity (>50%). These results suggest that the SVM output signals can be very useful for representing two-levels of classification results. The first level being a traditional hard cover type label and second representing pixel purity and associated classification accuracies. Users should be cautious in the interpretation of classification accuracy for pixels with high level of heterogeneity. It should be noted that the pixel purity label can also be generated for other classification

Table 4
Comparison of error matrix using homogenous and heterogeneous pixels for training data. Results are from SVM classification using 800 training pixels per class. Overall accuracy, Kappa coefficients, and the total number of sample points are highlighted in bold.

	Reference					
	Urban	Forest	Ag	Total	% Correct	% Commission
Pure						
Urban	**2.2**	1.4	1.8	5.4	41	59
Forest	1.6	**58.6**	7.9	68.1	86	14
Ag	1.0	6.2	**19.4**	26.5	73	27
Total%	4.8	66.1	29.1	100.0	**80**	(***n*** **= 71,063**)
% Correct	46	89	67			
% Omission	54	11	33			**Kappa = 0.58**
Mixed						
Urban	**2.2**	1.3	1.5	5.0	43	57
Forest	1.4	**56.8**	6.3	64.4	88	12
Ag	1.2	8.0	**21.2**	30.5	70	30
Total%	4.8	66.1	29.1	100.0	**80**	(***n*** **= 71,063**)
% Correct	45	86	73			
% Omission	55	14	27			**Kappa = 0.59**

algorithm. For instance, the strength of neural network output signals can be directly linked to sub-pixel cover type proportions (Moody et al., 1996; Foody, 1996).

4.3. SVM classification of heterogeneous pixels

Our initially selected training samples can be considered as "homogeneous" pixels. All training pixels had one dominant pixel cover type (i.e., 100%). This type of sampling scheme may not reflect the spectral variability of individual cover types (Gong and Howarth, 1990; Huang et al., 2002). Alternatively, there was the concern that SVM classification may be sensitive to outliers in the training set, since the optimal hyperplane of SVM was developed using only a small portion of the training data (Bishop, 2006).

An additional experiment was conducted by selecting training pixels including some heterogeneous pixel cover type proportions (i.e., dominant cover >75%). This sample scheme represented a relaxation of signal purity. The training, classification, and accuracy assessment procedures remained the same for the SVM classification. The inclusion of heterogeneous pixels in the training did not have large impacts on the overall accuracies and Kappa coefficients. Differences were within 1% with or without the inclusion of heterogeneous pixels in training (Table 4). The inclusion of heterogeneous pixels in the training data did result in more agricultural pixels (31.2%) than using homogeneous pixels for training (agricultural pixel = 26.4%). Accordingly, the commission error for agricultural land increased slightly (27% vs. 30%) and the omission error reduced from 33% to 27%. Overall, the similarity of classification performance using homogenous or heterogeneous pixels is promising for operational mapping efforts. In practice, training pixels can be selected with some flexibility, particularly when visual interpretation of MODIS time-series data is used for the training sample selection (Shao et al., 2010).

4.4. Regional scale operational classifications

The comparison of three classification algorithms clearly shows the superior classification accuracy of SVM versus the other two algorithms tested. Additional consideration for algorithm selection includes model parameters, speed, and easy-of-use. The CART algorithm has advantages in all of these aspects. It does not require additional model parameters and is fast in both training and actual data classification. The major problem is relatively low classification accuracies (Liu and Wu, 2005). The CART algorithm splits the feature space into many independent regions and each input is associated with one of these regions which are aligned with the axes of the feature dimension. This type of decision boundary is not smooth and the solution may not be the optimal (Bishop, 2006). Furthermore, the interpretability of CART is often overstated. The tree structure developed for many remote sensing classification applications can be very complex and it is impossible to derive meaningful interpretation.

SVM and NN both need to adjust additional model parameters. For the MLP NN classifier, we adjusted the number of nodes at the hidden layer, learning rate, momentum, and training epochs. Fig. 4 shows the impacts of network architecture (number of nodes at

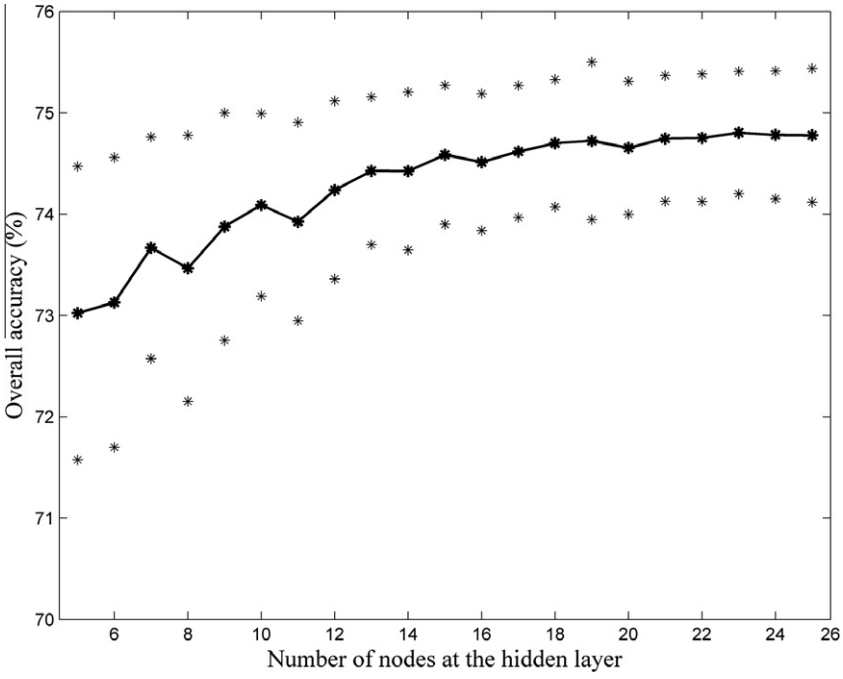

Fig. 4. The impacts of neural network architecture (number of nodes at the hidden layer) on classification results. The central line is the mean accuracy values from the 50 different repetitions. The boundary line represents mean value ± one standard deviation.

Table 5
Comparison of overall classification performance (APES, 2009) for the SVM, NN, and CART algorithms using a range of training data sample sizes.

	Sample size of training data									
	20	50	100	200	300	400	500	600	700	800
SVM	79.4	80.7	80.9	82.0	82.4	82.0	82.6	82.3	82.6	82.5
NN	73.7	76.9	78.0	80.6	81.4	82.1	82.2	82.3	82.3	82.7
CART	64.4	71.1	73.4	76.3	76.0	78.0	77.5	77.8	77.1	77.6

the hidden layer) for the classification. Other model parameters (i.e., learning rate and momentum) were kept stable for this testing. Overall accuracy values were derived from 50 different repetitions using 800 training pixels per class. The mean and standard deviation of overall accuracy were then calculated and compared. The overall accuracy continued increasing when the number of nodes at the hidden layer increased from 5 to 20 (at single node increments). However, there was no gain in the overall accuracy beyond 20 nodes. Different combinations of the model parameters lead to a large number of trials for network training. This is the major drawback of NN classifier, although NN typically generate good classification results if large numbers of training samples are available. For the SVM algorithm, only two model parameters (C and γ) were examined in our study. A grid-search algorithm was developed and limited human interactions were needed. The SVM training and classification can be time-consuming for a large remote sensing dataset. For this study, the SVM training time was not an issue because of the moderate sample size. The actual classification took several hours on a SUN Ultra 2 workstation. Given its classification performance, the SVM should be the superior algorithm for regional level land-cover characterization.

We employed the SVM algorithm for the classification of multiple year MODIS time-series data at annual intervals. We implemented the SVM classifications for 2001 and 2009 MODIS data. Two TM images from 2009 were obtained for the validation purpose. The TM imagery was classified using similar classification scheme and method used for the NLCD 2001 data (Homer et al., 2004). The classification results were degraded to 250 m spatial resolution. Each reference pixel was then labeled based on the dominate sub-pixel cover type proportion. We followed the same training, validation, and accuracy procedures used for the MODIS 2001 classification. Table 5 shows the accuracy assessment for 2009 MODIS classification using three different algorithms. SVM generated overall accuracies ranging from 79% to 83% for training sample sizes from 20 to 800 pixels per class, compared to 74% to 83% and 64% to 78% for NN and CART, respectively. Similar to the 2001 MODIS classification, SVM algorithm was superior when a relatively small number of training samples was used for the training. The overall accuracy was almost identical for SVM and NN algorithms when the number of training samples increased above 400 pixels per class. The results from CART were consistently lower compared to those obtained from other two algorithms.

5. Conclusions

Three classification algorithms were compared using MODIS time-series data as inputs. The classification experiments were conducted with respect to the impacts of training sample sizes, training sample variations, and the characteristics of reference data points. The SVM achieved higher overall accuracies and significantly improved Kappa coefficients for the entire range of training sample sizes compared to the NN and the CART algorithms. The differences were particularly large for smaller training sample sizes. Also, SVM classification performance exhibited minimal variability in response to different training data. Furthermore, classification accuracies were highly dependent on reference data characteristics. Overall accuracies differed significantly for reference pixels with homogeneous versus heterogeneous sub-pixel cover components. The SVM were implemented for the APES study area at the annual interval using MODIS time-series data. For a three-class classification scheme, the best overall accuracies were 80% and 83% for 2001 and 2009, respectively. For 2001 MODIS classification, overall three-class accuracies increased to 91% for SVM-derived "functionally homogeneous" pixels.

Acknowledgements

The authors would like to thank Dr. Lorenzo Bruzzone for his thoughtful suggestions in support of this study. Funding was partially provided under EPA's Global Earth Observation System of Systems (GEOSS) Advanced Monitoring Initiative (AMI) Grant #35. The US Environmental Protection Agency funded and conducted the research described in this paper. It has been subject to the Agency's programmatic review and has been approved for publication. Mention of any trade names or commercial products does not constitute endorsement or recommendation for use.

Notice: The US Environmental Protection Agency funded and conducted the research described in this paper. It has been subject to the Agency's programmatic review and has been approved for publication. Mention of any trade names or commercial products does not constitute endorsement or recommendation for use.

References

Bagan, H., Wang, Q.X., Watanabe, M., Yang, Y.H., Ma, Jianwen., 2005. Land cover classification from MODIS EVI times-series data using SOM neural network. International Journal of Remote Sensing 26 (22), 4999–5012.

Bishop, C.M., 2006. Pattern recognition and machine learning, first ed. Springer.

Bovolo, F., Camps-Valls, G., Bruzzone, L., 2010. A support vector domain method for change detection in multitemporal images. Pattern Recognition Letter 31 (10), 1148–1154.

Breiman, L., Friedman, J.H., Olshen, R.A., Stone, C.J., 1984. Classification and regression trees. Wadsworth International Group, Belmont, California.

Brown, M., Lewis, H.G., Gunn, S.R., 2000. Linear spectral mixture models and support vector machines for remote sensing. IEEE Transactions on Geoscience and Remote Sensing 38 (5), 2346–2360.

Camps-Valls, G., Bruzzone, L., 2005. Kernel-based methods for hyperspectral image classification. IEEE Transactions on Geoscience and Remote Sensing 43 (6), 1351–1362.

Camps-Valls, G., Gomez-Chova, L., Calpe-Maravilla, J., Martin-Guerrero, J.D., Soria-Olivas, E., Alonso-Chorda, L., Moreno, J., 2004. Robust support vector method for hyperspectral data classification and knowledge discovery. IEEE Transactions on Geoscience and Remote Sensing 42 (7), 1530–1542.

Camps-Valls, G., Gomez-Chova, L., Munoz-Mari, J., Rojo-Alvarez, J.L., Martinez-Ramo, M., 2008. Kernel-based framework for multitemporal and multisource remote sensing data classification and change detection. IEEE Transactions on Geoscience and Remote Sensing 46 (6), 1822–1835.

Carpenter, G.A., Gjaja, M.N., Gopal, S., Woodcock, C.E., 1997. ART neural networks for remote sensing: Vegetation classification from Landsat TM and terrain data. IEEE Transactions on Geoscience and Remote Sensing 35 (2), 308–325.

Carrão, H., Gonçalves, P., Caetano, M., 2008. Contribution of multispectral and multitemporal information from MODIS images to land cover classification. Remote Sensing of Environment 112 (3), 986–997.

Chen, J., Jonsson, P., Tamura, M., Gu, Z., Matsushita, B., Eklundn, L., 2004. A simple method for reconstructing a highquality NDVI time-series data set based on the Savitzky–Golay filter. Remote Sensing of Environment 91 (3–4), 332–344.

Defries, R.S., Townshend, J.R.G., 1994. NDVI-Derived land-cover classification at a Global-scale. International Journal of Remote Sensing 15 (17), 3567–3586.

Foody, G.M., 1996. Relating the land-cover composition of mixed pixels to artificial neural network classification output. Photogrammetric Engineering and Remote Sensing 62 (5), 491–499.

Foody, G.M., Mathur, A., 2004. A relative evaluation of multiclass image classification by support vector machines. IEEE Transactions on Geoscience and Remote Sensing 42 (6), 1335–1343.
Friedl, A.F., McIver, D.K., Hodges, J.C.F., Zhang, X.Y., Muchoney, D., Strahler, A.H., Woodcock, C.E., Gopal, S., Schneider, A., Cooper, A., Baccini, A., Gao, F., Schaaf, C., 2002. Global land cover mapping from MODIS: algorithms and early results. Remote Sensing of Environment 83 (1–2), 287–302.
Giri, C., Zhu, Z.L., Reed, B., 2005. A comparative analysis of the Global Land Cover 2000 and MODIS land cover data sets. Remote Sensing of Environment 94 (1), 123–132.
Gong, P., Howarth, P.J., 1990. An assessment of some factors influencing multispectral land-cover classification. Photogrammetric Engineering and Remote Sensing 56 (5), 597–603.
Gopal, S., Woodcock, C., Strahler, A., 1999. Fuzzy ARTMAP classification of global land cover from the 1 degree AVHRR data set. Remote Sensing of Environment 67 (2), 230–243.
Gualtieri, J.A., Cromp, R.F., 1999. Support vector machines for hyperspectral remote sensing classification. In: Proc. SPIE 27th AIPR Workshop: Advances in Computer Assisted Recognition, Washington DC, 14–16 October, pp. 221–232.
Hansen, M.C., DeFries, R.S., Townshend, J.R.G., Carroll, M., Dimiceli, C., Sohlberg, R.A., 2003. Global percent tree cover at a spatial resolution of 500 m: first results of the modis vegetation continuous fields algorithm. Earth Interactions 7, 1–15.
Homer, C., Huang, C., Yang, L., Wylie, B., Coan, M., 2004. Development of a 2001 national land-cover database for the United States. Photogrammetric Engineering & Remote Sensing 70 (7), 829–840.
Huang, C., Davis, L.S., Townshend, J.R.G., 2002. An assessment of support vector machines for land cover classification. International Journal of Remote Sensing 23 (4), 725–749.
Huete, A., Didan, K., Miura, T., Rodriguez, E.P., Gao, X., Ferreira, L.G., 2002. Overview of the radiometric and biophysical performance of the MODIS vegetation indices. Remote Sensing of Environment 83 (1–2), 195–213.
Joachims, T., 2002. Learning to classify text using support vector machines: methods, theory and algorithms. Springer.
Knight, J.F., Lunetta, R.S., Ediriwickrema, J., Khorrarn, S., 2006. Regional scale land cover characterization using MODIS-NDVI 250 m multi-temporal imagery: A phenology-based approach. Giscience & Remote Sensing 43 (1), 1–23.
Lawrence, R.L., Wright, A., 2001. Rule-based classification systems using classification and regression tree (CART) analysis. Photogrammetric Engineering & Remote Sensing 67 (10), 1137–1142.
Liu, W.G., Wu, E.Y., 2005. Comparison of non-linear mixture models: Sub-pixel classification. Remote Sensing of Environment 94 (2), 145–154.
Lobell, D.B., Asner, G.P., 2004. Cropland distributions from temporal unmixing of MODIS data. Remote Sensing of Environment 93 (3), 412–422.
Loveland, T.R., Reed, B.C., Brown, J.F., Ohlen, D.O., Zhu, Z., Yang, L., Merchant, J.W., 2000. Development of a global land cover characteristics database and IGBP DISCover from 1 km AVHRR data. International Journal of Remote Sensing 21 (6–7), 1303–1330.
Lunetta, R.S., Alvarez, R., Edmonds, C.M., Lyon, J.G., Elvidge, C.D., Bonifaz, R., García, C., Gómez, G., Castro, R., Bernal, A., Cabrera, A.L., 2002. NALC/Mexico land cover mapping results: implications for assessing landscape condition. International Journal of Remote Sensing 23 (16), 3129–3148.
Lunetta, R.S., Shao, Y., Ediriwickrema, J., Lyon, J.G., 2010. Monitoring agricultural cropping patterns across the Laurentian Great Lakes Basin using MODIS-NDVI data. International Journal of Applied Earth Observation and Geoinformation 12 (2), 81–88.
Lunetta, R.S., Knight, J.F., Ediriwickrema, J., Lyon, J.G., Worthy, L.D., 2006. Land-cover change detection using multi-temporal MODIS NDVI data. Remote Sensing of Environment 105 (2), 142–154.
Moody, A., Gopal, S., Strahler, A.H., 1996. Artificial neural network response to mixed pixels in coarse-resolution satellite data. Remote Sensing of Environment 58 (3), 329–343.
Mountrakis, G., Im, J., Ogole, C., 2011. Support vector machines in remote sensing: A review. ISPRS Journal of Photogrammetry and Remote Sensing 66 (3), 247–259.
Melgani, F., Bruzzone, L., 2004. Classification of hyperspectral remote sensing images with support vector machines. IEEE Transactions on Geoscience and Remote Sensing 42 (8), 1778–1790.
Nowak, D.J., Greenfield, E.J., 2010. Evaluating the National Land Cover Database tree canopy and impervious cover estimates across the conterminous United States: A comparison with photo-interpreted estimates. Environmental Management 46 (3), 378–390.
Pal, M., Mather, P.M., 2005. Support vector machines for classification in remote sensing. International Journal of Remote Sensing 26 (5), 1007–1011.
Paola, J.D., Schowengerdt, R.A., 1995. A detailed comparison of backpropagation neural network and maximum-likelihood classifiers for urban land-use classification. IEEE Transactions on Geoscience and Remote Sensing 33 (4), 981–996.
Quinlan, J.R., 1993. C4.5: programs for machine learning. Morgan Kaufmann Publishers, San Mateo, CA.
Richards, J.A., Jia, X.P., 1999. Remote sensing digital image analysis: an introduction. Springer.
Shao, Y., Lunetta, R.S., Ediriwickrema, J., Iiames, J., 2010. Mapping cropland and major crop types across the Great Lakes Basin using MODIS-NDVI data. Photogrammetric Engineering & Remote Sensing 76 (1), 73–84.
Shao, Y., Lunetta, R.S., 2011. Sub-pixel mapping of tree canopy, impervious surfaces, and cropland in the Laurentian Great Lakes Basin using MODIS time-series data. IEEE Journal of Selected Topics in Applied Earth Observations and Remote Sensing 4 (2), 336–347.
Tasdemir, T., Merenyi, E., 2009. Exploiting data topology in visualization and clustering of self-organizing maps. IEEE Transactions on Neural Networks 20 (4), 549–562.
Townshend, J.R.G., Justice, C.O., 2002. Towards operational monitoring of terrestrial systems by moderate-resolution remote sensing. Remote Sensing of Environment 83 (1–2), 351–359.
Vapnik, V.N., 1995. The nature of statistical learning theory. Cambridge University Press, New York.
Vapnik, V.N., 1998. Statistical Learning Theory. Wiley, New York.
Venables, W.N., 1997. Modern applied statistics with S-PLUS, 2nd ed. Springer, New York.
Wardlow, B.D., Egbert, S.L., Kastens, J.H., 2007. Analysis of time-series MODIS 250 m vegetation index data for crop classification in the US Central Great Plains. Remote Sensing of Environment 108 (3), 290–310.
Wardlow, B.D., Egbert, S.L., 2008. Large-area crop mapping using time-series MODIS 250 mNDVI data: An assessment for the US Central Great Plains. Remote Sensing of Environment 112 (3), 1096–1116.
Wickham, J.D., Stehman, S.V., Fry, J.A., Smith, J.H., Homer, C.G., 2010. Thematic accuracy of the NLCD 2001 land cover for the conterminous United States. Remote Sensing of Environment 114 (6), 1286–1296.
Xavier, A.C., Rudorff, B.F.T., Shimabukuru, Y.E., Berka, L.M.S., Moreira, M.A., 2006. Multi-temporal analysis of MODIS data to classify sugarcane crop. International Journal of Remote Sensing 27 (4), 755–768.
Xiao, X.M., Boles, S., Liu, J.Y., Zhuang, D.F., Frolking, S., Li, C.S., et al., 2005. Mapping paddy rice agriculture in southern China using multi-temporal MODIS images. Remote Sensing of Environment 95 (4), 480–492.
Zell, A., 1998. SNNS Stuttgart Network Simulator. User Manual, Version 4.2, University of Tübingen, Wilhem-Schickerd-Institute for Computer Science.